

A Study on Blends of Different Molecular Weights of Polypropylene

B. L. DEOPURA and S. KADAM,* *Textile Technology Department, Indian Institute of Technology, Delhi, New Delhi 110016, India*

Synopsis

Blends of small percentage of plastic grade polypropylene with fiber grade polypropylene are studied in unoriented and oriented states. A 3% blend sample has a higher spherulitic growth rate, and improved mechanical behavior in drawn fiber state as compared to the parent sample. These changes are related to the presence of bimodal and trimodal crystal texture of polypropylene in the blend, respectively. At a higher blend percent, specifically at 10 and 15%, the mechanical properties of the drawn fiber are inferior and these are related to partial phase segregation of the components.

INTRODUCTION

There are a few reports on studies of blends of different molecular weights of polypropylene (PP). Blends of different fractions of PP¹ showed lower impact resistance; however, the processing of such blends was superior to the PP of comparable intrinsic viscosity. Blends of PP resins² were found to have better spinning performance for fine denier fibers than those prepared from individual resins.

Blends of poly(ethylene oxide) samples of different molecular weights were studied by Cimmino et al.³ and observed phase segregation during casting of films. Mechanical properties did not show any particular trend with blend ratio. Hinrichsen and Green⁴ studied the rheological behavior of blends of two different molecular weights of nylon 6 and found that the processing of a high molecular weight component can be improved by blending low molecular weight at specified ratios. Similar observations were made by Bhateja and Andrews⁵ regarding processing of ultrahigh molecular weight linear polyethylene when blended with normal molecular weight linear polyethylene; however, the mechanical properties were found to be intermediate between that of parent samples.

Addition of small amounts of nylon 11 was found to improve the mechanical properties in comparison with 100% PP fibers.⁶ A study on blends of nylon 6 and nylon 66^{7,8} showed that a small percent of either of the components significantly changes the crystallization behavior of the major component. Even 3% of nylon 66 changes the nylon 6 α -crystal form to γ -form during the process of melt spinning and it also improves the fiber properties.

The present investigation deals with the blends of fiber grade PP and a small percentage of plastic grade PP with a view to study the crystallization

* Present address: J. K. Synthetics, Kota-324 003, India.

behavior in an unoriented state and mechanical properties in an oriented fiber state.

EXPERIMENTAL

The two kinds of polypropylene chips selected were low molecular weight fiber grade IPXL XF-81 (LMPP) and high molecular weight plastic grade IPCL S-1730 (HMPP). Characteristics of the control samples are given in Table I. Melt flow index was measured as flow rate (g) for 10 mm at 230°C under a load of 2.16 kg. Intrinsic viscosity of the samples were measured in Decalin at 135°C and viscosity average molecular weights were calculated.

Four blend samples were prepared by melt extrusion with LMPP, containing 3,5,10, and 15 wt % of HMPP. Rheological behavior of the samples was investigated by Instron Capillary Rheometer Model 1112 at four different strain rates of 29, 118, 588, and 1176 cm^{-1} , L/D ratio of 20, and temperature of 250°C. Spherulitic growth rate studies were conducted at 133°C from melt (at 200°C for 1 min) in a polarizing microscope attached with Mettler hot stage. Small-angle light scattering experiments were done on samples crystallized at 133°C in a silicon oil bath from melt. Spherulitic radii were obtained from the scattering patterns.

A laboratory model melt spinning unit was used for production of a monofilament with spinning temperatures in the range of 250–270°C. A two stage drawing was carried out for these filaments with a first stage draw ratio of 1.4 at 50°C and the rest in the second stage at 90°C. All the spun samples were drawn to three sets of draw ratios, i.e., 6,7, and samples drawn to a maximum draw (MDR). The drawn filaments were heat set at 100°C for 30 min in a fixed length condition for further experiments.

Wide angle X-ray diffraction studies were carried out for isothermally crystallized thin films (at 133°C) and for spun and drawn samples. The crystalline orientation function was calculated with the help of (110) and (040) X-ray reflections using the Wilchinsky⁹ relation for a monoclinic system. X-ray crystallinity for drawn fibers was obtained from X-ray diffractometer scans of powdered samples.

Birefringences were measured for drawn filaments using a Vickers polarizing microscope with a Leitz Wetzler tilting-plate type compensator. The amorphous orientation function (f_a) was calculated using the Stein and Norris¹⁰ method in a manner applied to PP by Samuels.¹¹ Phase contrast microscopy experiments were done for MDR samples.

RESULTS AND DISCUSSION

The melt viscosity vs. blend ratio at four shear rates are shown in Figure 1. It is observed that, at low shear rates, there is a large increase in melt viscosity even with a small addition of HMPP, whereas at high shear rates,

TABLE I
Characteristics of Polypropylene Chips

Sample code	M F I (g)	I Y (dL/g)	\bar{M}_v
IPCL XF-81 (LMPP)	14.0	1.26	119,000
IPCL S-1730 (HMPP)	1.7	2.80	322,000

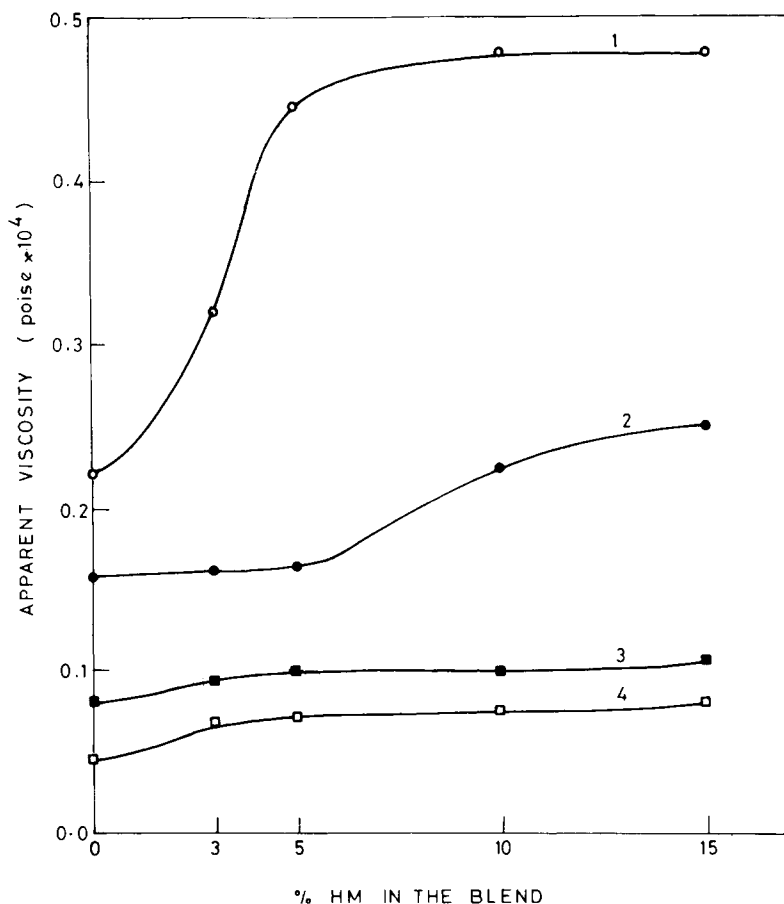


Fig. 1. Apparent viscosity as a function of % HM in the blend at constant shear rate of (1) 29, (2) 118, (3) 588, and (4), 1176 s^{-1} and at a temperature of 250°C.

which are actually observed during melt spinning, the rise in the viscosity is marginal. These changes are attributed to the orientation of long HMPP molecular chains at high shear rates.

Figure 2 shows the changes in the spherulite radius, with time for isothermally crystallized samples, and a representative set of volume filled spherulites are shown in Figure 3. It is observed that the growth rate for an HMPP sample is much lower than that of LMPP. It is well known that with increasing molecular weight the transport of macromolecules to the surface of the growing crystals is hindered, and this results in reduction of the spherulitic growth rate. Linear growth rates for 3% HM sample shows that HMPP molecules in the blend are a part of the lamellae or are entrapped in interfibrillar channels. At a higher percentage of HMPP, non-linear growth rates are observed.

The nonlinearity in the spherulitic growth rates implies that the concentration of HMPP at the types of radial fiber goes on increasing with increasing spherulitic size. This accounts for (a) increasing openness of the spherulitic texture as defined by the ratio (δ) of the diffusion coefficient in the melt and the radial growth rate of the spherulites and (b) diffuse bound-

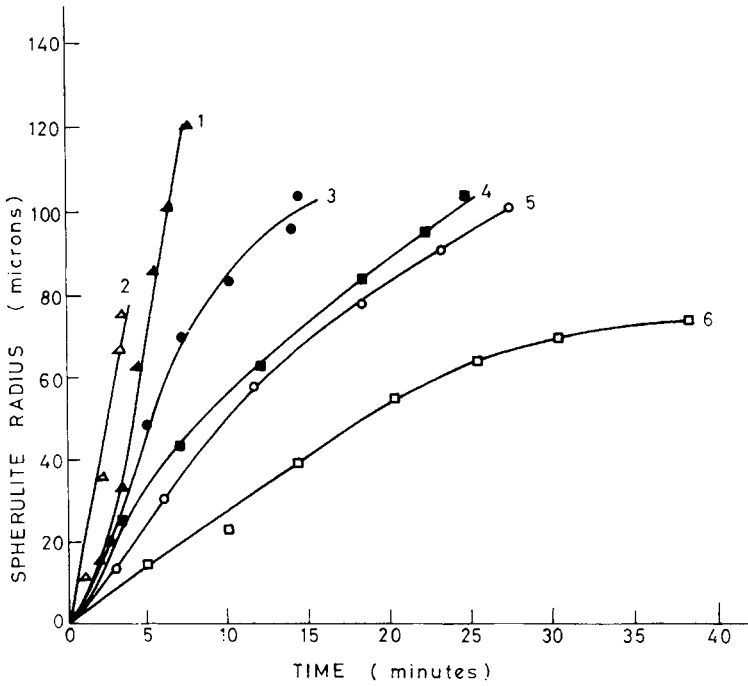


Fig. 2. Spherulite radius as a function of time for isothermally crystallized samples. HM (%): (1) 0; (2) 3; (3) 5; (4) 10; (5) 15; (6) 100.

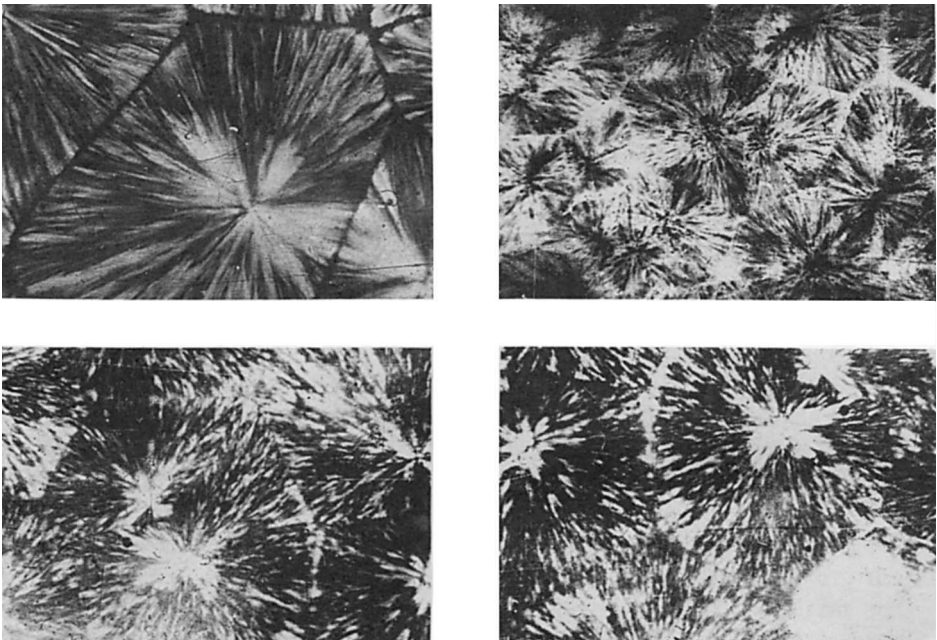


Fig. 3. Volume-filled spherulites for (a) LMPP, (b) 3% HM (c) 5% HM, and (d) 10% HM samples.

aries at the surface of the spherulites as observed by the photographs in Figure 3. Lovinger¹² observed that the addition of up to 10% high density polyethylene in PP decreases the spherulitic growth rates, and the rates become nonlinear.

Normal four-lobed H_v small-angle light scattering patterns were observed for isothermally crystallized films at 133°C. The spherulite sizes as obtained from SALS pattern are given in Table II and are nearly equal to the sizes obtained from spherulitic growth rate data. It is most interesting to note the 3% HM sample has a fourfold nucleation density (calculated from spherulite sizes), as compared to the LMPP sample. It appears that some highly resistant crystalline regions of HMPP in the blend act as a nucleating agent for the LMPP sample.

Figure 2 shows that the spherulitic growth rate for 3% HM sample is greater than the LMPP sample. As a result of changes in nucleation and grow rates, the overall crystallization rate (at the initial stages of spherulitic growth) for 3% HM at 133°C is observed to be almost 14 times the corresponding value for the LMPP sample.

Wide angle X-ray diffraction patterns of the isothermally crystallized samples are shown in Figure 4. A visual comparison of intensity distribution for (110), (040), and (130) reflections with % HM shows that the relative intensities for (110) and (130) reflections are higher for 3% HM than that for the LMPP sample while the corresponding intensities are lower for blends at a higher percentage. These changes in X-ray intensity are related to the presence of bimodal crystal texture of PP^{6,13-22} in blends with *c*- and *a*-axis crystal orientations with a reference direction.

Anderson and Carr¹⁵ found a greater percentage of second population crystallites (with *a*-axis parallel to the fiber axis) in melt-spun fibers than in the hot-drawn films. They proposed two possible explanations for bimodal crystal texture, (a) geometrical constraints placed on crystallization interlamellar material and (b) epitaxial attachment of chains to a growing lamellar crystallite. They favored the latter explanation.

They¹⁵ proposed a growth model for flow-crystallized PP based on epitaxial deposition. It was suggested that nucleation and initial growth of primary population lamellae oriented perpendicular to the flow direction occurs as a result of the chains being oriented parallel to the flow direction. Extended chain tie molecules between vertically adjacent lamellae would be the load bearing linkages, and, consequently, the major flow stresses would be transmitted through the system by the stakes of parallel lamellae

TABLE II
Spherulite Radius as Measured from Small-Angle Light Scattering

Blend composition (% HMPP)	Spherulite radius (μm)
0	109
3	64
5	83
10	90
15	86
100	61

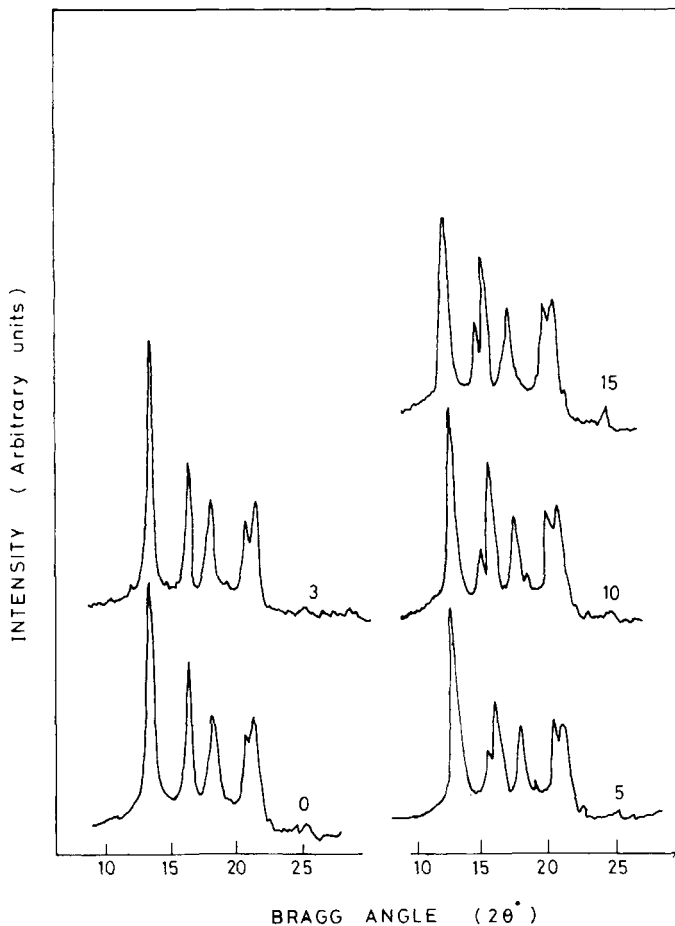


Fig. 4. Wide-angle X-ray diffraction patterns for isothermally crystallized samples (1) LMPP, (2) 3% HM, (3) 5% HM, (4) 10% HM, and (5) 15% HM.

crystallites. At the perimeter of the laterally growing lamellae there will be a zone of relatively relaxed melt in which chains will not be subjected to strong orientation effects and could permit epitaxial nucleation leading to bimodal texture.

For the 3% HM sample, the addition of HMPP molecules in LMPP may induce tie chains between the lamellae during the growing spherulites even when few orientation effects are present. These tie chains could permit nucleation of second population crystallites. This supports the explanation offered for flow crystallized PP.¹⁵ For samples with higher HM percent, the HMPP molecules are preferentially rejected from the spherulites, as discussed earlier.

An additional X-ray diffraction peak in Figure 4 is observed for 5, 10, and 15% HM blends at 2θ of $\sim 16^\circ$. This is related with (100) reflection of β -crystal form for PP.²³ The second peak at 2θ of 21.9° for β -form gives rise to variation of intensity in the doublet at 21.1° and 21.9° of α -form. The presence of β -crystal form has been related to the fractions containing a high degree of isotacticity and observed in strongly birefringent spheru-

lites.²⁴ However, the presence of such a crystal form in the blend system is not easily explained. Possibly, the presence of HMPP chains impart some kind of a disturbance and does not allow the crystallization to occur in α -form. Similar changes in the crystal forms have been observed for nylon 6 when blended with a small percentage of nylon 66.^{7,8}

Some representative wide-angle X-ray diffraction photographs are shown in Figure 5. The as-spun LMPP sample has a bimodal crystal texture [Fig. 5(a)], and it is seen that second population crystallites are higher than the first one, which confirms earlier observations¹⁵ for similar samples. Further, the percentage of second population crystallites increases [Fig. 5(b)] with % HM as observed by intensity distribution of the (110) plane. This shows that HMPP molecules are also responsible for generating bimodal texture in addition to the stresses during spinning. Seth and Kempster⁶ observed that addition of even 5% nylon 11 significantly increases the

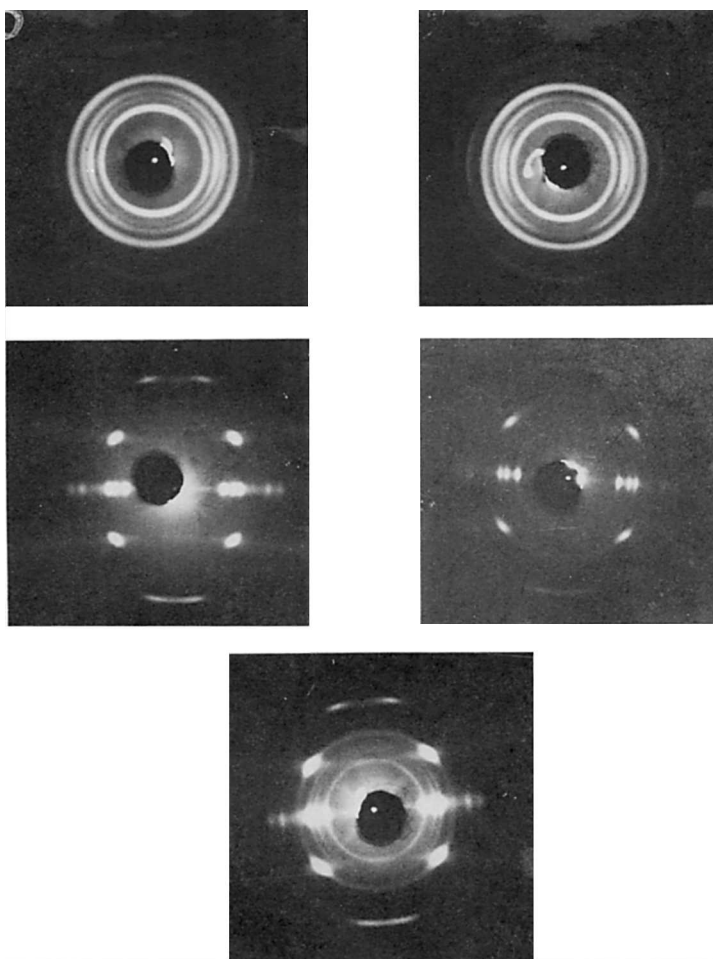


Fig. 5. Fiber X-ray diffraction photographs for (a) as-spun LMPP, (b) as-spun 3% HM, (c) drawn LMPP, (d) drawn 3% HM, and (e) drawn 15% HM samples.

second population crystallites in as-spun PP, although the reasons for such an observation in the present case are similar to those discussed above.

Fiber X-ray diffraction photographs for drawn LMPP and 3 and 15% HM samples are shown in Figures 5(c)–(e), respectively. It is observed that the drawn LMPP sample has a unimodal crystal texture with *c*-axis parallel to the fiber axis. However, for blends, in addition to a relatively high first orientation mode, there are other orientations present. A close look at the intensity variations of (110) diffraction [Figs. 5(d) and 5(e)] shows that, in addition to intense maxima at the equator, there are a couple of small maxima, which may possibly correspond to the trimodal crystal texture observed earlier^{6,13} [particularly Fig. 1(d) of Ref. 6]. Such a texture is further supported by the intensity distribution of (130) diffraction arcs [Figs. 5(d) and 5(e)]. It is also seen that the population of second and third orientation modes increases with % HM.

These observations indicate that, for blends, HMPP chains do not allow all the second population crystallites, in the as-spun (undrawn) blend sample, to orient along the fiber axis during drawing. The presence of the third orientation mode in the drawn sample may have several origins, i.e., (a) the third orientation is present in the as-spun sample and is not observed in the diffraction pattern due to its relatively small fraction, (b) the third orientation mode has been described as a tilted first orientation mode,^{13,15} and thus it may be generated from first (or second) orientation mode during drawing due to the presence of HMPP chains.

X-ray crystallinity, birefringence, crystalline (f_c), and amorphous (f_a) orientation functions for MDR samples are given in Table III. The 3 and 5% HM samples show distinctly high birefringence values. The f_c values are calculated assuming the *c*-axis parallel to the fiber axis and thus are approximate for blends. The f_c and f_a values indicate that the increased birefringence for 3 and 5% blends are related to increases in amorphous orientation. Similar increases in amorphous orientation has been observed for several fiber blend systems with a small percentage of minor component.^{6,8,13,25}

Tenacity, yield stress, and initial modulus for MDR samples are plotted as a function of % blend composition in Figure 6. It is observed that 3% HM sample shows distinctly high modulus and tenacity. This is observed to be true for set of samples with draw ratios of 6 and 7 as well.²⁷ The improved mechanical behavior for 3% HM sample is related to a combination of the factors, i.e., (a) increased amorphous orientation, (b) HMPP

TABLE III
X-Ray Crystallinity, Birefringence, Crystalline, and Amorphous Orientation
for MDR Samples

Blend composition (% HMPP)	Crystallinity (%)	Δn	f_c	f_a
0	63	0.032	0.92	0.75
3	64	0.035	0.95	0.87
5	60	0.035	0.92	0.88
10	65	0.033	0.94	0.79
15	51	0.032	0.94	0.71

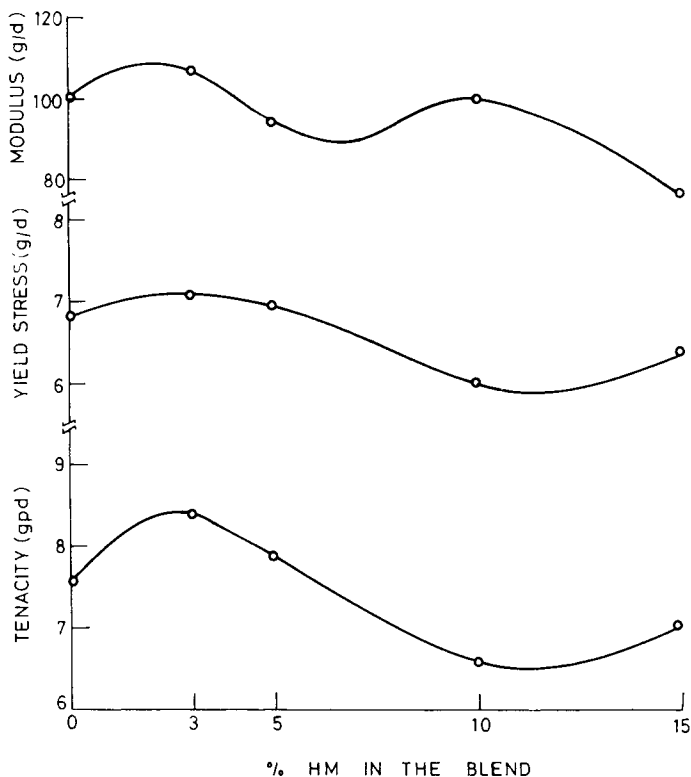


Fig. 6. Tenacity, yield stress, and modulus as a function of percent HM.

molecules acting as tie chains, and (c) a possible reduction in crystal size with the addition of HMPP molecules in the blend.

The relatively inferior mechanical behavior for 10 and 15% HM samples are related to lower amorphous orientation, which may occur due to partial phase segregation. Two representative phase contrast micrographs in Figure 7 for 3 and 15% HM samples show increasing contrast between skin and core, with % HM in the blend. Further experiments are in progress to ascertain this fact.

CONCLUSIONS

Bimodal crystal texture and β -crystal form have been observed for spherulites of LMPP blended with HMPP. An increase in the spherulitic growth rate for the 3% HM sample is related to the presence of bimodal crystal texture. The HMPP molecules also act as a nucleating agent for LMPP at the 3% level.

Drawn LMPP sample has a unimodal crystal texture whereas blend fibers seem to show a trimodal texture. The anchored HMPP molecules do not allow complete conversion of bimodal to unimodal texture for drawn blends. Improved mechanical behavior for the 3% HM sample are related to higher amorphous orientation and HMPP molecules acting as tie chains. Inferior mechanical properties for 10 and 15% HM samples are related to partial phase segregation of the components.

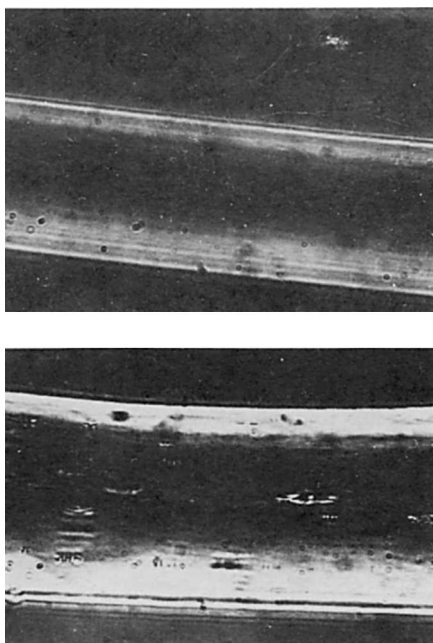


Fig. 7. Phase contrast micrographs for (a) 3% HM and (b) 15% HM samples.

We are thankful to M/s IPCL, Baroda and Neomer, Baroda for supplying the PP chips. We also thank the Bombay Textile Research Association, Bombay, for allowing us to use their phase-contrast microscopy system.

References

1. J. Van Schooten, H. Van Hoorn, and J. Boerma, *Polymer*, **2**, 161 (1961).
2. R. L. Hudson, Chevron Research Co., U.S. Pat. 4296022.
3. S. C. Cimmino, R. Greco, E. Martuscelli, and L. Nicolais, *Polymer*, **19**, 1079 (1978); *Makromol. Chem.*, **180**, 219 (1979).
4. G. Hinrichsen and W. Green, *Hunststoffe*, **71**, 2 (1981).
5. S. K. Bhateja and E. H. Andrews, *Polym. Eng. Sci.*, **12**, 888 (1983).
6. K. K. Seth and C. J. E. Kempster, *J. Polym. Sci., Polym. Symp.*, **58**, 297 (1977).
7. B. L. Deopura, Anu Verma, and A. K. Sengupta, *Man Made Tex.*, **26**, 539 (1983).
8. Anu Verma, B. L. Deopura, and A. K. Sengupta, *J. Appl. Polym. Sci.*, to appear.
9. Z. W. Wilchinsky, *J. Appl. Phys.*, **30**, 792 (1959).
10. R. S. Stein and F. H. Norris, *J. Polym. Sci.*, **21**, 381 (1961).
11. R. J. Samuels, *J. Polym. Sci.*, **A3**, 174 (1965).
12. A. Lovinger, *J. Appl. Polym. Sci.*, **25**, 1703 (1980).
13. A. Halim, Ph.D. thesis, University of Manchester, U.K., 1980.
14. K. Katayama, T. Ameno, and K. Nakamura, *Kolloid Z. Z. Polym.*, **226**, 125 (1968).
15. P. G. Anderson and S. H. Carr, *J. Mater. Sci.*, **10**, 870 (1975).
16. M. Compostella, A. Coen, and F. Bertinotti, *Angew. Chem.*, **74**, 618 (1964).
17. H. Awaya and N. H. Zasshi, *Nippon Kagaku Zasshi*, **82**, 1575 (1961).
18. Z. Menaik and D. L. Fitchmun, *J. Polym. Sci.*, **A11**, 973 (1973).
19. V. I. Selikhova, Yu A. Zubov, G. S. Markova, and V. A. Kargin, *Vysokomol. Soyed.*, **7**, 216 (1965).
20. F. Khoury, *J. Res. NBS 70A (Phys. and Chem) No. 1*, 29 (1966).
21. F. J. Padden, Jr., and H. D. Keith, *J. Appl. Phys.*, **44**, 1217 (1973).
22. F. L. Bisbergen and B. G. M. Delange, *Polymer*, **9**, 23 (1968).

23. E. J. Addink and J. Beintema, *Polymer*, **2**, 185 (1961).
24. H. D. Keith, F. J. Padden Jr., N. N. Walter, and H. W. Wyckoff, *J. Appl. Phys.*, **30**, 1485 (1959).
25. B. L. Deopura and K. Sankar, unpublished data.
26. K. K. Seth, Ph.D. thesis, University of Manchester, U.K., 1976.
27. S. Kadam, M. Tech. thesis, Indian Institute of Technology, New Delhi, 1985.

Received June 21, 1985

Accepted September 6, 1985